

## Analysis and design of demountable steel column-baseplate connections

Dongxu Li<sup>\*1</sup>, Brian Uy<sup>1,2a</sup>, Farhad Aslani<sup>3b</sup> and Vipul Patel<sup>4c</sup>

<sup>1</sup> Centre for Infrastructure Engineering and Safety, School of Civil and Environmental Engineering, The University of New South Wales, Sydney, NSW 2052, Australia

<sup>2</sup> School of Civil Engineering, The University of Sydney, Sydney, NSW 2006, Australia

<sup>3</sup> School of Civil, Environmental and Mining Engineering, The University of Western Australia, Crawley, WA 6009, Australia

<sup>4</sup> School of Engineering and Mathematical Sciences, College of Science, Health and Engineering, La Trobe University, P.O. Box 199, Bendigo, VIC 3552, Australia

(Received June 21, 2016, Revised October 10, 2016, Accepted October 24, 2016)

**Abstract.** This paper aims to investigate the demountability of steel column-baseplate connections subjected to monotonic and cyclic loading. This paper presents the finite element analysis of steel column-baseplate connections under monotonic and cyclic loading. The finite element model takes into account the effects of material and geometric nonlinearities. Bauschinger and pinching effects were also included in the developed model, through which degradation of steel yield strength in cyclic loading can be well simulated. The results obtained from the finite element model are compared with the existing experimental results. It is demonstrated that the finite element model accurately predicts the initial stiffness, ultimate bending moment strength of steel column-baseplate connections. The finite element model is utilised to examine the effects of axial load, baseplate thickness, anchor bolt diameter and position on the behaviour of steel column-baseplate connections. The effects of various parameters on the demountability of steel column-baseplate connections are investigated. To achieve a demountable and reusable structure, various design parameters need to be considered. Initial stiffness and moment capacity of steel column-baseplate connections are compared with design strengths from Eurocode 3. The comparison between finite element analysis and Eurocode 3 indicates that predictions of initial stiffness for semi-rigid connections should be developed and improved design of the connections needs to be used in engineering practice.

**Keywords:** steel columns; column-baseplate connections; monotonic and cyclic loading; demountability; finite element analysis

### 1. Introduction

In recent years, many newly constructed buildings have been demolished due to their inability to be dismantled or meet the needs for new owners. As reported by the Green Building Council of Australia (2009), approximately 40% of landfill waste can be attributed to building and

---

\*Corresponding author, Ph.D. Student, E-mail: [d.li@unsw.edu.au](mailto:d.li@unsw.edu.au)

<sup>a</sup> Professor, E-mail: [b.uy@unsw.edu.au](mailto:b.uy@unsw.edu.au)

<sup>b</sup> Senior Lecturer, E-mail: [farhad.aslani@uwa.edu.au](mailto:farhad.aslani@uwa.edu.au)

<sup>c</sup> Lecturer, E-mail: [v.patel@latrobe.edu.au](mailto:v.patel@latrobe.edu.au)

construction. The large amount of greenhouse gas emissions have encouraged measures, such as reducing and reusing constructional materials, to be carried out. The steel column-baseplate connection is one of the most important structural elements in steel frames, which is normally used to transfer axial forces, shear forces and moments from the superstructure into the foundation. Steel column-baseplate connections can generally be utilised with either rigid or pinned constraints. These connections are categorised into the exposed bolted system and embedded system. Most of the steel column-baseplate connections utilised in low to medium rise steel structures are based on the exposed bolted system (Grauvalardell *et al.* 2005). For the exposed bolted steel column-baseplate connections, steel columns are welded on top of baseplates, which are then connected to concrete foundations with a number of anchor bolts.

Experimental, numerical and analytical studies on the behaviour of column-baseplate connections with the exposed bolted system are conducted. Picard and Beaulieu (1985) tested a series of column-baseplate connections with various column sections. Test results indicate that axial compressive forces significantly increase the flexural stiffness of column-baseplate connections. Nakashima (1992) conducted tests on steel tubular column-baseplate connections subjected to bending and shear. It was found that the column-baseplate connection with a small section exhibited significant differences in rigidity and durability. Targowski *et al.* (1993) experimentally investigated the behaviour of the baseplates of column-baseplate connections with various column sections. The deformation of baseplate at different positions was recorded and yield line of baseplate was identified to modify the analytical model. Jaspart and Vandegans (1998), Gomez *et al.* (2010) and Stamatopoulos and Ermopoulos (2011) performed extensive experiments on the column-baseplate connections. It was found that anchor bolts and baseplates dominate the behaviour of column-baseplate connection.

From an analytical point of view, Wald *et al.* (1995, 1996) proposed analytical models with a component method to predict the initial stiffness and flexural bending moment capacity of column-baseplate connection. The research findings are included into the Eurocode 3. Jaspart and Vandegans (1998) proposed a mechanical model for predicting the initial stiffness and bending moment capacity of the column-baseplate connections. The comparison between experimental and analytical results indicate that the column-baseplate connection exhibits highly semi-rigid behaviour, even for the pinned constraints. Stamatopoulos and Ermopoulos (2011) derived an analytical formula for the prediction of the behaviours of column-baseplate connection according to the correlation between experimental results and finite element analysis. Compared to experimental and analytical studies, limited literatures have been found to investigate behaviours of column-baseplate connections with finite element analysis. Stamatopoulos and Ermopoulos (2011) and Kanvinde *et al.* (2013) developed a finite element model with a focus on the prediction of initial stiffness of the column-baseplate connection. Finite element analysis for accurately predicting the cyclic behaviours of a column-baseplate connection is rarely found.

The above literature review demonstrates that studies on demountability of steel column-baseplate connections have not been conducted. The concept of demountable connections was first presented by Uy (2014) who suggested that the steel column and connections could deform elastically without undergoing large plastic deformation, which results in the reuse of steel columns after their useful service life. This paper presents finite element models using ABAQUS (2012) for predicting the behaviours of steel column-baseplate connections under monotonic and cyclic loading. Experimental results from literature were used to verify the finite element model. Extensive finite element analysis is conducted thereafter to provide an in-depth understanding into the concepts of demountable steel column-baseplate connections.

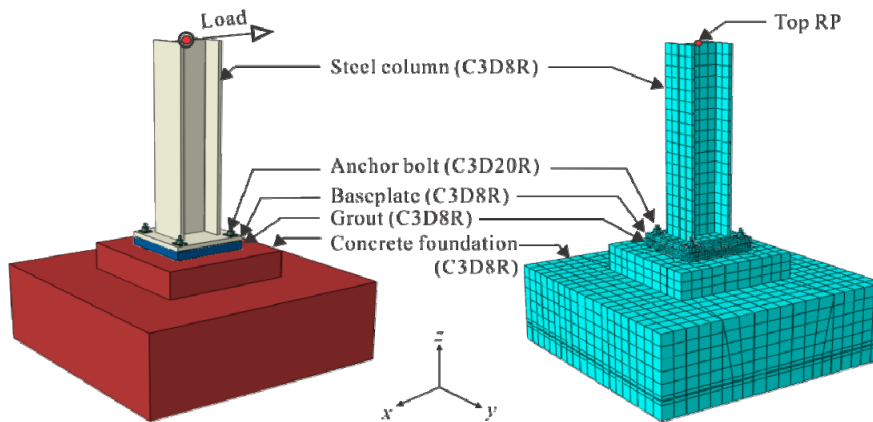


Fig. 1 Steel column-baseplate connections with finite element mesh

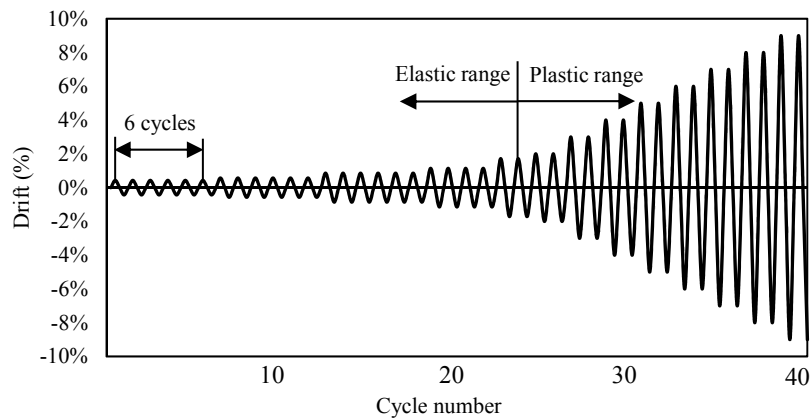


Fig. 2 Typical loading protocol for steel structures in cyclic loads (ATC-24)

## 2. Finite element model of column-baseplate connection

### 2.1 Basic concept

Full-scale tests can be used to obtain the most reliable behaviour of steel column-baseplate connections, nevertheless, they are time consuming and expensive to examine the effects of every parameter of the behaviour of steel column-baseplate connections. To propose a procedure for the design of steel column-baseplate connection, limited experimental data is insufficient. The finite element analysis package ABAQUS (2012) is employed for the nonlinear analysis of steel column-baseplate connections.

### 2.2 Mesh, boundary condition and loading

In this study, all parts of the test specimens, which include steel columns, baseplates, anchor bolts, grout and concrete foundations were modelled with three-dimensional solid elements. A typical finite element model of a column-baseplate connection is depicted in Fig. 1(a). In addition,

8-node linear brick elements with reduced integration (C3D8R) were utilised to simulate steel columns, baseplates, grout and concrete foundations to reduce the computational time. A 20-node quadratic brick element with reduced integration (C3D20R) was employed for simulating anchor bolts due to their ability to capture the stress concentration more effectively and accurately, which was suggested by Mirza and Uy (2011).

In the finite element model, appropriate mesh size ensures the accuracy and efficient analysis time of the finite element model. In this paper, a mesh sensitivity study was conducted to provide a rational mesh size for each modelling part (Fig. 1(b)). Based on the sensitivity analysis, the mesh size of the column section was determined to be  $L/30$ , in which  $L$  represents the column height. It was found that the stress concentration around bolts is significant, therefore a finer mesh size for the baseplate and grout was taken as  $B_p/20$  and  $B_g/20$ , where  $B_p$  and  $B_g$  is the width of the baseplate and grout, respectively. The concrete foundation has limited effect on the test results; therefore, mesh size was determined as  $B_c/15$ , with  $B_c$  representing the width of the concrete foundation.

Bottom ends of the steel column-baseplate connections were constrained with fix-ended boundary conditions. All nodes on the top surface of steel column were tied with a centrally located reference point. The axial loads and horizontal deformation was applied to the top reference point. In particular, ATC-24 (1992) cyclic loading history with 40 cycles was applied in the horizontal direction of top reference point, which was specifically developed for components of steel structures. This loading protocol shown in Fig. 2 was one of the formal protocols developed for seismic performance evaluation for steel structures.

### 2.3 Interactions between components

Surface-to-surface contact with a Hard Contact model in the normal direction with no penetration was considered for all contact surfaces. A Coulomb friction model in the tangential direction was assumed with a friction coefficient. The appropriate value of friction coefficient depends on the material of contacted components and treatment of surfaces (Eurocode 3 2005). In this analysis, friction coefficients between steel-to-steel components and steel-to-concrete components were assigned as 0.3 and 0.6, respectively.

The surfaces, which come into contact (Fig. 3) and are assigned as surface-to-surface contact, are the inner surface of the washer to the top surface of the baseplate (Contact A), the anchor

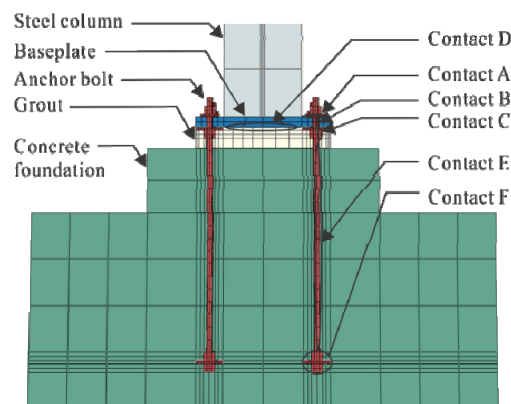


Fig. 3 Interactions of the FE model

shank to the bolt hole (Contact B), the outer surface of the levelling nut and the washer to the grout (Contact C), the bottom surface of baseplate to grout or concrete foundation (Contact D), the bolt shank to surrounding concrete foundation (Contact E), as well as the outer surface of nut and washer to surrounding concrete foundation (Contact F). Moreover, ‘‘Tie’’ constraints were utilised to simulate interactions between the steel column-to-baseplate and grout-to-concrete foundation.

## 2.4 Material properties

### 2.4.1 Concrete for monolithic behaviour

In this analysis, a damage plasticity model defined in ABAQUS was used to simulate concrete behaviour in compression and tension. Concrete material parameters required to be defined include elastic modulus ( $E_c$ ), Poisson's ratio ( $\nu_c$ ), flow potential eccentricity ( $e$ ), viscosity parameter, dilation angle ( $\psi$ ), shape factor for yield surface ( $K_c$ ), the ratio of initial equibiaxial compressive yield stress to initial uniaxial compressive yield stress ( $f_{b0}/f'_c$ ). As suggested by ACI (2008), Poisson's ratio is adopted as 0.2 and the elastic modulus of concrete is determined from  $E_c = 3320f'_c{}^{0.5} + 6900$ , where  $f'_c$  is in MPa. Flow potential eccentricity ( $e$ ) is taken as 0.1 and viscosity parameter is determined to be 0.001. For dilation angle ( $\psi$ ),  $40^\circ$  is normally used,  $f_{b0}/f'_c$  equals to  $1.5(f'_c)^{-0.075}$  and  $K_c = 5.5/[5 + 2(f'_c)^{0.075}]$  (Aslani *et al.* 2015).

Equivalent stress-strain relationships of concrete in compression and tension are also desired. The compressive equivalent stress-strain curve illustrated in Fig. 4 was used to simulate the compressive behaviour of concrete, which was proposed by Carreira and Chu (1985), where the stress in compression is assumed to be linear up to a value of  $0.4f'_c$ . Beyond this point, the stress is represented as a function of strain

$$\sigma_c = \frac{f'_c \gamma (\varepsilon_c / \varepsilon'_c)}{\gamma - 1 + (\varepsilon_c / \varepsilon'_c)^\gamma} \quad (1)$$

where  $\gamma = |f'_c/32.4|^3 + 1.55$  and  $\varepsilon'_c = 0.002$ .

Tensile behaviour of concrete is assumed to be linear until the tensile strength is reached, which is taken as  $0.56(f'_c)^{0.5}$ . Beyond this failure stress, the tensile response is represented by fracture energy ( $G_F$ ). Fracture energy can be calculated through the following equation

$$G_F = (0.0469d_{\max}^2 - 0.5d_{\max} + 26) \left( \frac{f'_c}{10} \right)^{0.7} \quad (2)$$

where  $d_{\max}$  represents the maximum coarse aggregate size in mm and it is taken as 20 mm.

### 2.4.2 Structural steel for monolithic behaviour

The stress-strain characteristics of steel column, baseplate and anchor bolt are essentially similar. Their behaviour is initially elastic after which yielding and strain hardening develop. The bilinear approach is found to be accurate to represent the stress-strain relationship. In addition, bilinear approach can better represent the hardening behaviour of the high-strength steel compared with trilinear approach. In this analysis, bilinear approach is utilised due to the use of high-strength anchor bolts and the behaviour of anchor bolt dominate the behaviour of the steel column-baseplate connections.

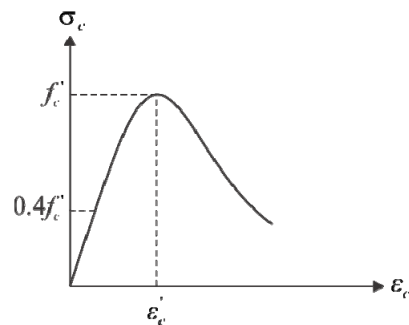


Fig. 4 Stress-strain relationship of concrete in compression

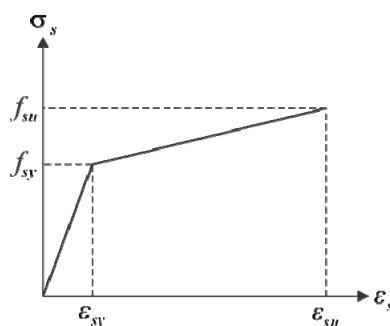


Fig. 5 Stress-strain relationship for structural steel in monolithic loading

### 2.4.3 Structural steel for cyclic behaviour

Under cyclic condition, properties of steel material are proved to be different from the monotonic condition by many researchers such as Bari and Hassan (2000), Jia and Kuwamura (2014) and Silvestre *et al.* (2015). Due to the Bauschinger effect, reversed yield stress was decreased and the hardening behaviour is strongly affected by the previous strain history. For the purpose of accurately predicting the behaviour of structural steel under cyclic loading, combined nonlinear kinematic and isotropic hardening model was utilised. In particular, Chaboche (1994) proposed a three-component nonlinear kinematic hardening rule based on Armstrong and Frederick (1966) one component approach. In this analysis, the complex three-component nonlinear kinematic rule and combined with isotropic hardening model was developed for structural steel. Bauschinger effect, pinching effect and ratcheting response can be well predicted.

According to Bari and Hassan (2000) and Jia and Kuwamura (2014), a series of parameters for various structural steel are determined. The accuracy of these parameter are ensured by comparing finite element analysis results with the independent experimental results. In Table 1,  $\sigma_0$  is the yield stress at zero plastic strain.  $Q$  represents the maximum change in the size of yield surface and  $b$  is the rate at which yield stress change with plastic strain.  $C_1$  to  $C_3$  are the kinematic hardening modulus and  $\gamma_1$  to  $\gamma_3$  represent the rate at which hardening modulus decrease with plastic strain.

Fig. 6 illustrates a general example of the stress-strain relationship for high-strength anchor bolt in cyclic loading, which was used in this analysis. Observed in Fig. 6, the hardening behaviour of structural steel is affected by the previous strain accumulation. The damage accumulation ensures the decreasing of yield stresses in the reversed cycles.

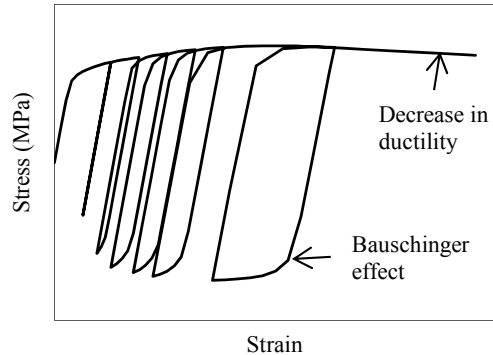


Fig. 6 Stress-strain relationship for structural steel in cyclic loading

## 2.5 Verification of finite element models

### 2.5.1 Monotonic loading

Most commonly used steel columns in column-baseplate connections include steel I-sections and hollow tubular sections (RHS, CHS). In this analysis, four specimens with various design details from Nakashima (1992), Targowski *et al.* (1993), Gomez *et al.* (2010) and Stamatopoulos and Ermopoulos (2011), were selected to evaluate the reliability of the developed finite element model. The geometry and material details are given in Fig. 7 and Table 2.

As shown in Fig. 8(a), experiment was stopped after yield bending moment was achieved and the deviation in initial stiffness was due to the unclear of axial loading history. Fig. 8(b) indicates that the finite element model can accurately predict the initial stiffness and bending moment capacity of the column-baseplate connection. For the transient part, initial stiffness from finite element analysis is slightly higher than the experimental result. This is because anchor bolt threads were not included in the developed finite element model, which consequently increases the strength of anchor bolts. In addition, there is a slight difference in the plastic part of the curves after yielding, which is due to the use of idealised behaviour of steel in stress-strain relationship. Fig. 8(c) indicates the finite element prediction agrees reasonably well with the experimental results. The slight difference in terms of initial stiffness may be attributed by the unclear position of the selected point, where rotation calculation was conducted. Due to the lack of moment-rotation curve from the experiment, moment-vertical displacement curve of a selected point was chosen for the comparison in Fig. 8(d). As observed, the predicted vertical displacement from the finite element model at the initial stage is smaller than the experimental results. This deviation was induced by the unclear of the real yield strength of anchor bolt.

Table 1 Parameters for combined hardening model for various structural steel

Element	Yield stress $\sigma_0$ (N/mm <sup>2</sup> )	Isotropic parameters			Kinematic parameters				
		$Q$ (N/mm <sup>2</sup> )	$b$	$C_1$	$\gamma_1$	$C_2$	$\gamma_2$	$C_3$	$\gamma_3$
Anchor bolt	750	210	35	55000	1100	15000	285	400	150
	320	150	4.5	76000	16500	6300	1250	400	385
Baseplate	280	140	3.5	65000	3500	26000	650	400	350
Steel column	350	150	6.5	57500	2250	4500	1100	100	70

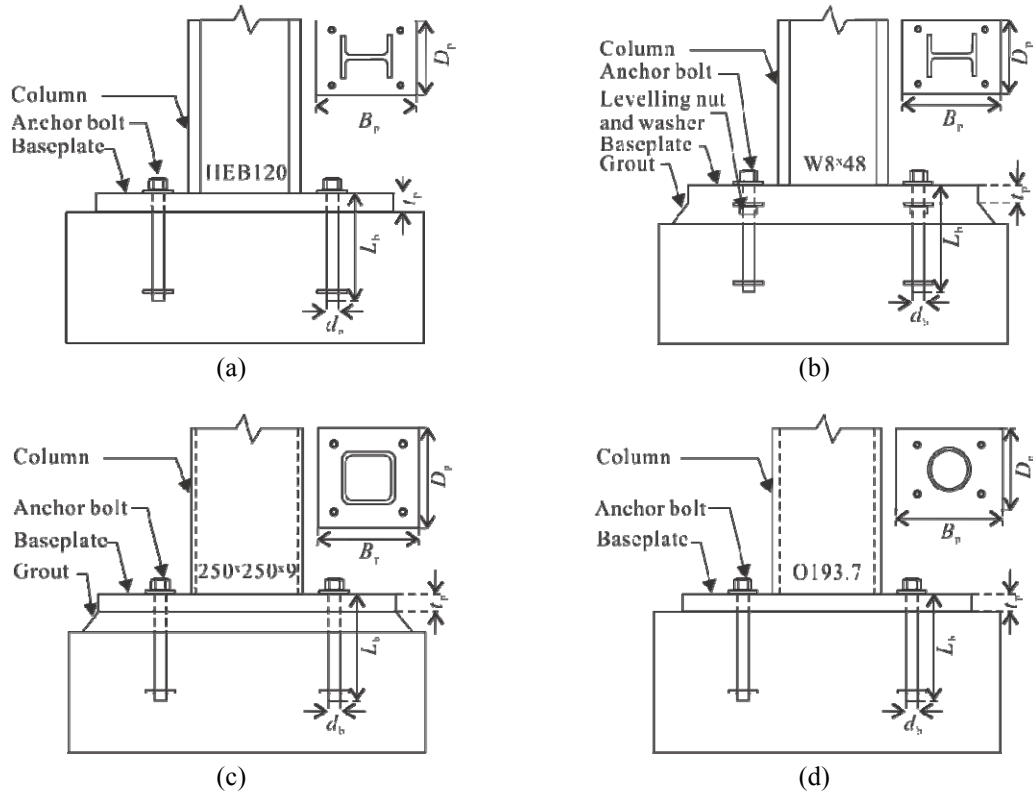


Fig. 7 Typical steel column-baseplate connections

Overall, results obtained from the finite element model agree well with the experimental data, and the deviation in the post-yielding region does not affect the accuracy of the finite element model because demountable connections only need to be simulated in the elastic region.

Table 2 Geometric and material property details

Specimen	Axial load $P$ (kN)	Baseplate dimension $(B_p \times D_p \times t_p)$ (mm)	Baseplate yield stress $f_{yp}$ (MPa)	Bolt $(d_b \times L_b)$ (mm)	Bolt yield stress $f_{yb}$ (MPa)	Strength of grout $f'_g$ (MPa)	Strength of concrete $f'_c$ (MPa)
SP1	198	240×140×16	416	12×340	460	-	29.2
Test 1	0	356×356×25.4	278	19×650	784	51	27
II-25-09	0	460×460×32	370	35×750	380	50	32
O193.7	0	400×300×10	370	24×630	320	-	50
Test 2	0	356×356×25.4	280	19×650	550	54.2	27.7
Test 4	411.5	356×356×38.1	250	19×650	335	63.7	29.3
Test 5	411.5	356×356×25.4	280	19×650	550	64.8	29.7
Test 7	678.4	356×356×25.4	280	19×650	550	65.3	30.3

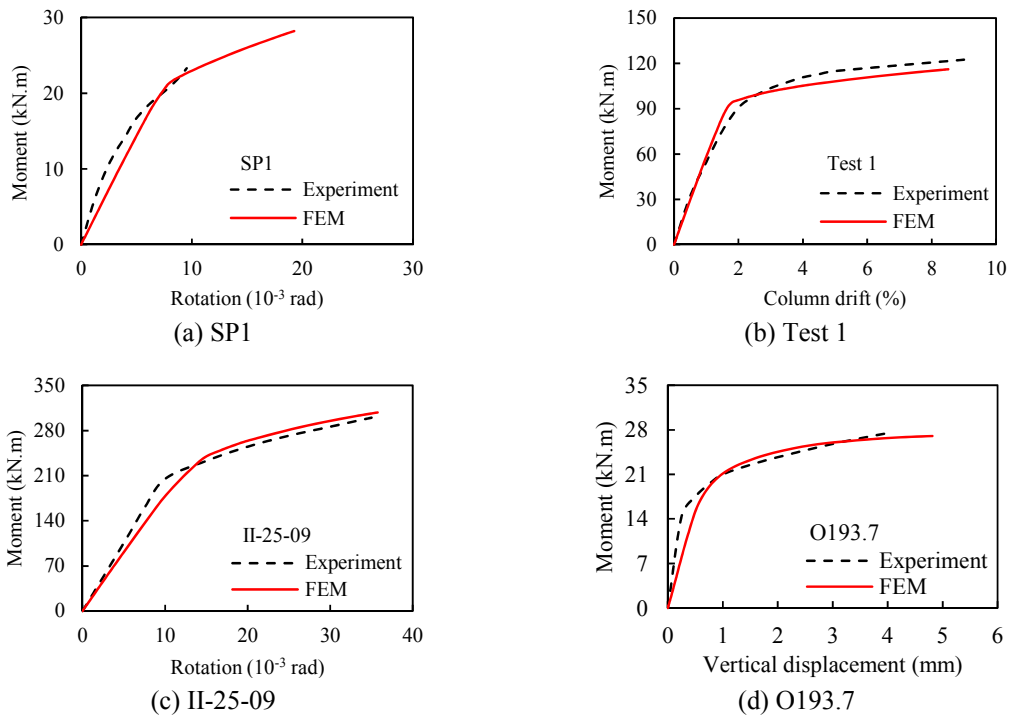


Fig. 8 Validation of FE models for various specimens under monotonic loading

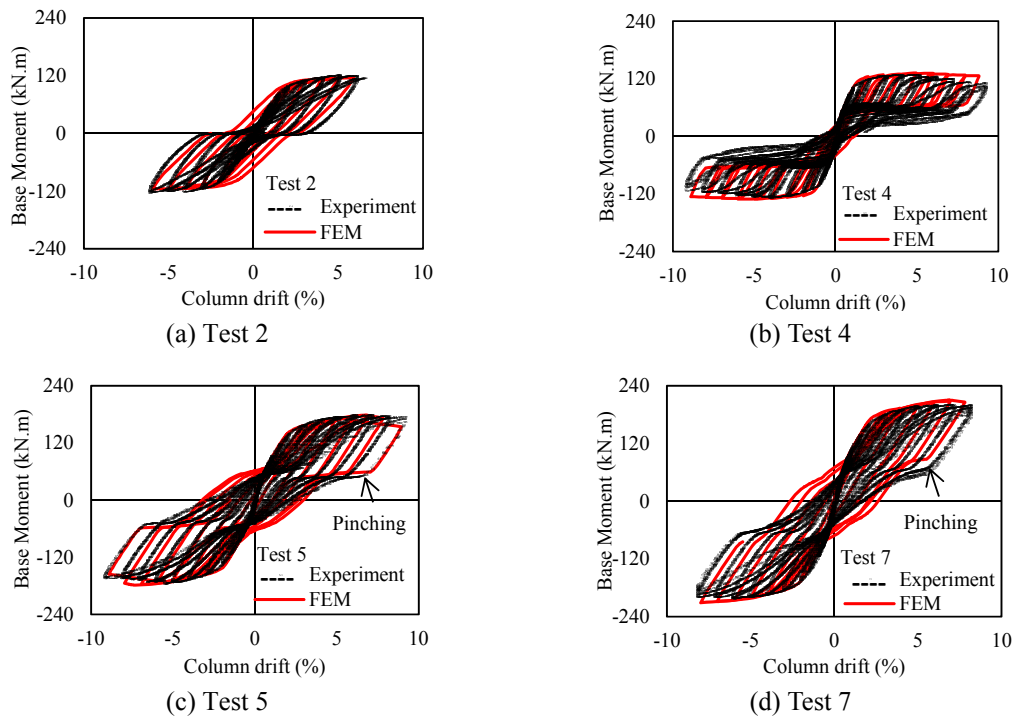


Fig. 9 Validation of FE models for various specimens under cyclic loading

### 2.5.2 Cyclic loading

Four sets of experimental results obtained from Gomez *et al.* (2010) were used to evaluate the accuracy of the developed finite element model in cyclic loading. The geometry of the steel column-baseplate connection is illustrated in Fig. 7(b) and varied parameter was given in Table 2. It can be seen from Table 2 that Tests 4 to 7 were subjected to different axial loads before horizontal cyclic deformation was applied. Moreover, Test 4 utilised a thicker baseplate of 38.1 mm but a smaller yield stress of 250 MPa.

Fig. 9 presents the comparison between experimental and finite element analysis results. As shown in the figure, finite element model predicts initial stiffness and ultimate bending moment capacity very well. Pinching effect can be observed in Figs. 9(c) and (d).

## 3. Parametric study

This section presents and discusses the results of parametric analysis on the monotonic and cyclic behaviour of steel column-baseplate connections using the developed finite element models. Compared with moment-rotation curves, moment-column drift curves do not need the selection of certain point along the column height. In addition, behaviours of steel column-baseplate connections such as initial stiffness and ultimate bending moment capacity can be obtained from moment-column drift curves. Therefore, following parametric study for the behaviours of column-baseplate connection was conducted on the basis of moment-column drift curves obtained from the developed finite element model. Moreover, for the ease of observation and comparison, envelope curves obtained from combining peak points of each cycle of moment-drift curves were presented for cyclic behaviours of column-baseplate connections.

In this analysis, parametric study of the main variables in a steel column-baseplate connection was carried out to examine the potential effects of a series of parameters. The authors herein take into account four different variables which include different axial loads, baseplate thicknesses, as well as anchor bolt positions and diameters. A course of analysis was conducted with one parameter varied each time according to Table 3 and the geometric details are illustrated in Fig. 10. It should be noted that in the following parametric study, the baseplate dimension is same with Test 1 in Table 2, which has a width and depth of 356 mm, respectively.

### 3.1 Effects of axial load

To study the effect of axial load, the finite element analysis with 0% to 40% of ultimate compressive capacity of the column ( $P_u$ ) was conducted. Fig. 11(a) shows the comparison of the moment-column drift curves obtained from the finite element analysis. As observed in Fig. 11(a), the increase in axial load can increase both the initial stiffness and ultimate moment capacity of the steel column-baseplate connection. For specimens with 10% and 20% of  $P_u$  applied on top of the column, the ultimate moment capacities were increased to 165 and 213 kN.m, respectively, which are 45% and 86% higher compared to the one with 0%  $P_u$  subjected to column (114 kN.m).

Fig. 11(b) shows the moment-column drift curves with differences in axial load. Similar to the monotonic loading, the increase in axial load increases the initial stiffness and ultimate bending moment capacity.

Failure modes for column-baseplate connection in monotonic and cyclic loading are similar. Fig. 12(a) presents the failure modes of column-baseplate connection with zero axial load, in which the ultimate strength of anchor bolt is higher than that of the connection with 20%  $P_u$ . Fig.

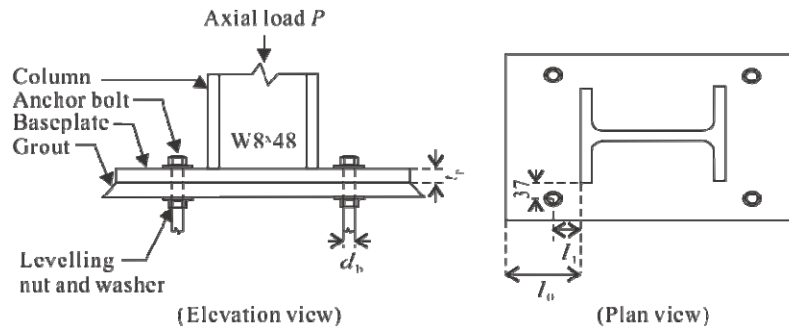


Fig. 10 Illustration of geometric details varied in parametric studies

Table 3 Details of parametric studies

Parameters	Values		
	0% $P_u$	10% $P_u$	20% $P_u$
Axial load on top of column $P$ (kN)			
Baseplate thickness $t_p$ (mm)	19.1	25.4	38.1
Anchor bolt position $l_1/l_0$	0.19	0.45	0.70
Anchor bolt diameter $d_b$ (mm)	19	24	28

12(b) indicates that when a column is subjected to a higher axial load (20%  $P_u$ ), more significant deformation of baseplate can be observed and less ultimate strength in anchor bolt is produced.

### 3.2 Effects of baseplate thickness

Fig. 13(a) depicts the comparison of the moment-column drift curves with different baseplate thickness. It can be observed that the ultimate moment capacity and initial stiffness would increase with an increase in baseplate thickness, which is within expectation as the yield of baseplate was delayed by using a thicker baseplate. In particular, the moment capacity was increased by 9.6% and 12.5% when increasing baseplate thickness from 16.9 to 25.4 and 38.1 mm, respectively. It is also found from finite element analysis that the behaviour of specimens with baseplate thickness beyond 38.1 mm is not changed. The initial stiffness and ultimate moment capacity were less affected due to yielding was not observed in baseplate and the behaviours of column-baseplate connections largely depend on the anchor bolt.

Fig. 13(b) compares the envelope curves with various baseplate thickness for column-baseplate connection in cyclic loading. It can be seen that there is slightly increase in the initial stiffness and ultimate bending moment capacity when increasing baseplate thickness, which is due to the yielding of baseplate was delayed by the use of thicker plate. However, it can also be observed that once a certain value of baseplate thickness was reached, the initial stiffness and ultimate bending moment capacity was less affected by the increase of baseplate thickness, which is similar to the behaviour of column-baseplate connection in monotonic loading.

Fig. 14 presents the failure modes for specimens with baseplate thickness of 16.9 and 38.1 mm. It can be seen in Fig. 14(a) that baseplate with small thickness deformed significantly and lower stress was produced on anchor bolts. For connection with a baseplate of 38.1 mm thick, less deformation was observed in the baseplate and higher stress was observed in tensile anchor bolts, which is shown in Fig. 14(b).

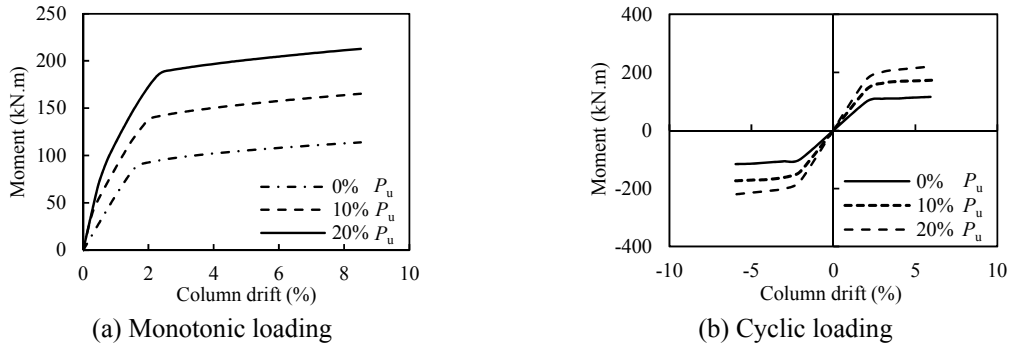


Fig. 11 Effects of axial loading on moment-column drift curves

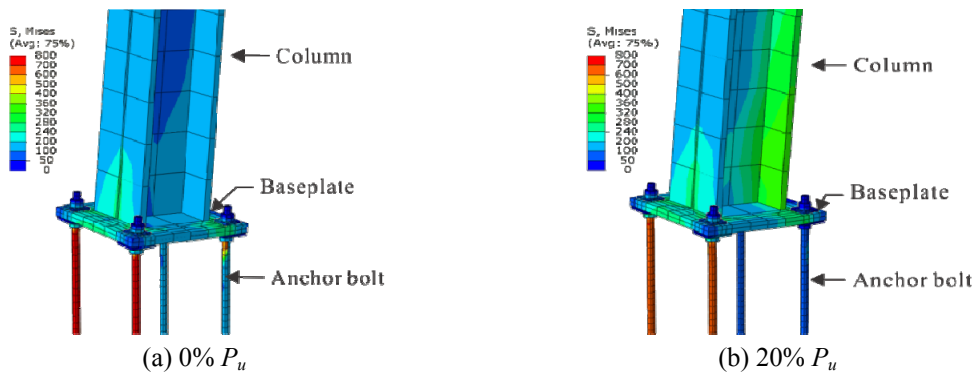


Fig. 12 Failure modes of column-baseplate connections with various axial load level

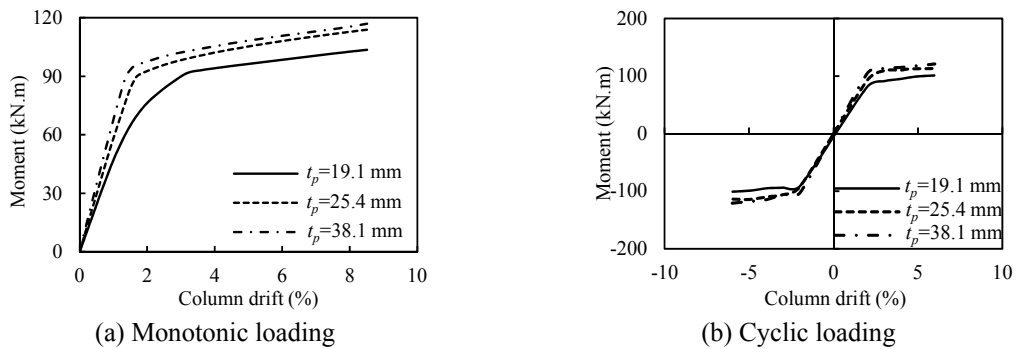


Fig. 13 Effects of baseplate thickness on moment-column drift curves

### 3.3 Effects of anchor bolt position

Three different anchor bolt positions were used in the parametric studies which included  $l_1/l_0 = 0.19, 0.45$  and  $0.70$ . The moment-column drift curves in Fig. 15(a) for different cases showed that there is no significant change in the initial stiffness. Nevertheless, further anchor bolt away from column flange results in a higher ultimate moment capacity. Fig. 15(a) also showed that

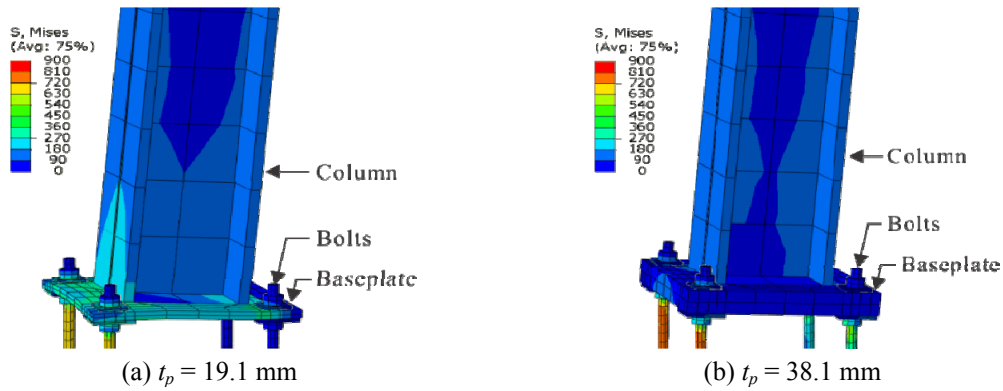


Fig. 14 Failure modes of column-baseplate connections with various baseplate thickness

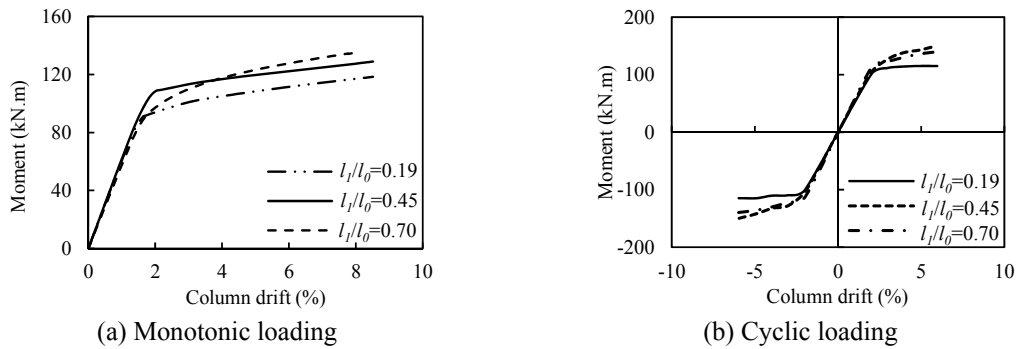


Fig. 15 Effects of anchor bolt position on moment-column drift curves

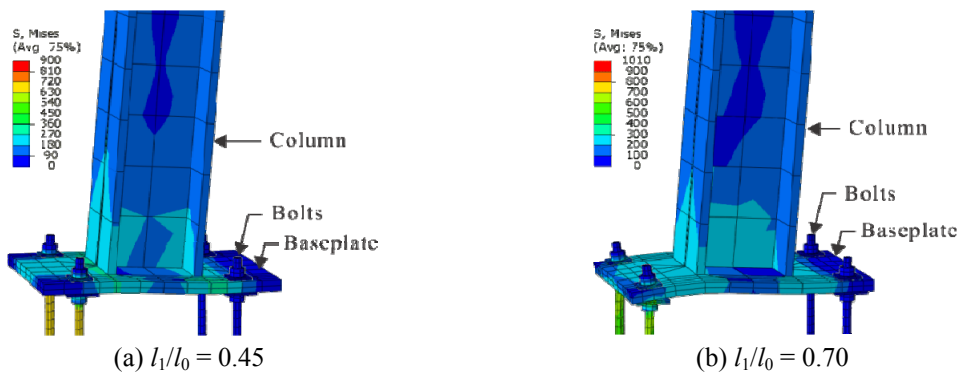


Fig. 16 Failure modes of column-baseplate connections with various anchor bolt position

connection with  $l_1/l_0 = 0.70$  would induce the yield of baseplate before the yield of the anchor bolt, which performed a curved transition part after yield.

For the effects of bolt position on the cyclic behaviour of column-baseplate connection. Conclusions from finite element analysis are similar to monotonic loading, initial stiffness were not significantly affected by the bolt position. However, arrange anchor bolts in the mid-span

between column flange and baseplate edge can achieve the largest yield bending moment capacity.

Fig. 16 presents the failure modes for specimens with  $l_1/l_0 = 0.45$  and  $0.70$  in finite element analysis. It can be observed in Fig. 16(a) that anchor bolts in tension sides had more stress and baseplate was less deformed. For specimen with anchor bolts close to baseplate short-span edge ( $l_1/l_0 = 0.70$ ), anchor bolts were subjected to less stress and baseplate deformed significantly, which is illustrated in Fig. 16(b).

### 3.4 Effects of anchor bolt diameter

In order to examine the effects of anchor bolt diameter on the moment-column drift curves, three different anchor bolt diameters were used in the parametric studies. The anchor bolt diameters varied from 19 to 28 mm. Fig. 17(a) shows a comparison of the moment-column drift curves with a difference in anchor bolt diameter. As shown in Fig. 17(a), the ultimate moment capacity was increased significantly by 46% and 71% when increasing the anchor bolt diameter from 19 to 24 and 28 mm, respectively. Moreover, the increase in anchor bolt diameter also increases the initial stiffness of steel column-baseplate connection.

Fig. 17(b) shows the envelope curves with differences in anchor bolt diameter. It can be found that an increase in anchor bolt diameter causes an increase in ultimate bending moment capacity and initial stiffness. As shown in Fig. 17(b), the ultimate moment capacity was increased

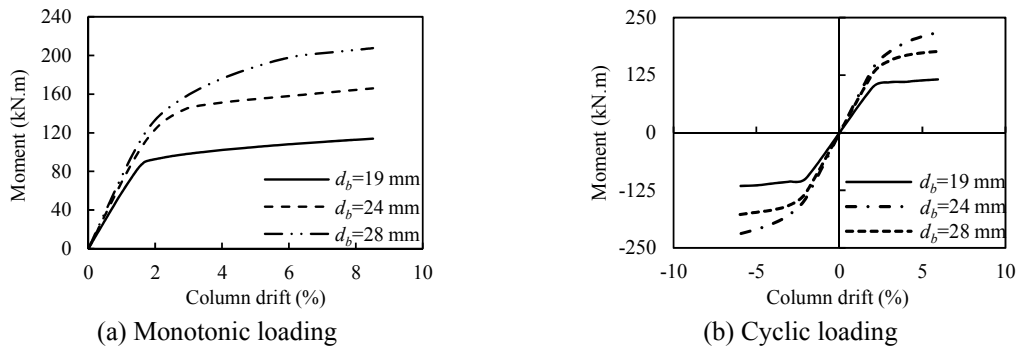


Fig. 17 Effects of anchor bolt diameter on moment-column drift curves

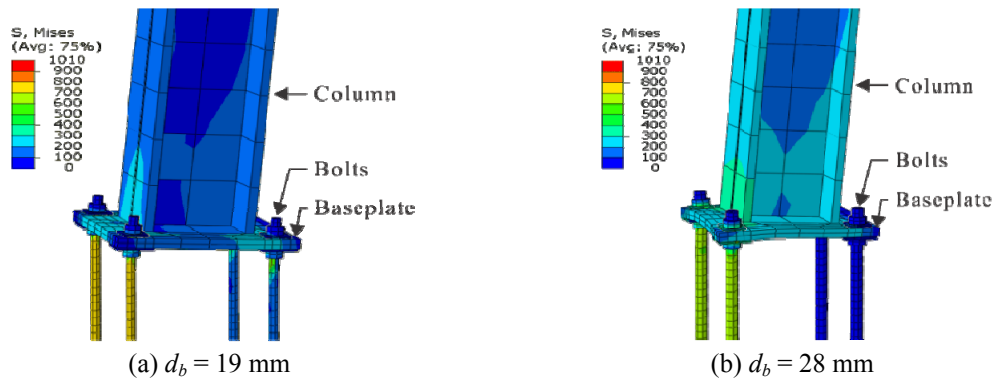


Fig. 18 Failure modes of column-baseplate connections with various anchor bolt diameter

significantly by 52% and 88% when increasing the anchor bolt diameter from 19 to 24 and 28 mm, respectively.

Failure modes are largely the same for column-baseplate connection in monotonic and cyclic loading. Fig. 18 illustrates the failure modes for specimens with an anchor bolt diameter of 19 and 28 mm. The use of smaller bolt diameter results in a higher stress in anchor bolts; meanwhile less deformation was formed in the baseplate. On the contrary, specimen with 28 mm bolt diameter leads to the less stress in anchor bolts and more significant deformation in baseplate.

#### 4. Plastic damage in steel column-baseplate connections

Uy *et al.* (2016) and Li *et al.* (2016) indicated that elasticity of a steel component is characterised by its ability to sustain elastic deformation without undergoing significant plastic deformation. The demountability of steel column-baseplate connection depends on the elasticity of steel column and baseplate. The demountability of steel column-baseplate connections cannot be achieved with large plastic deformation occurred in the column or baseplate.

Large plastic deformation in a column and baseplate for steel column-baseplate connections is illustrated in Fig. 19 and PEEQ represents a equivalent plastic strain. The moment-column drift curve for column-baseplate connection under monotonic and cyclic loading is presented in Fig. 20

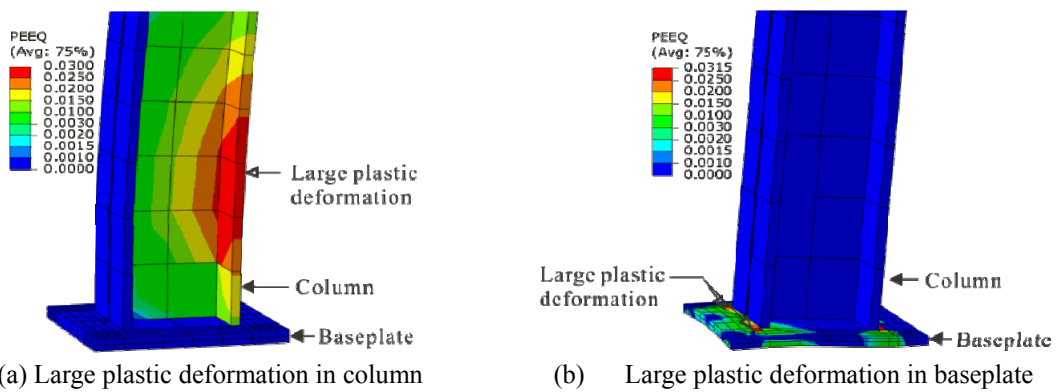


Fig. 19 Large plastic deformation of column and baseplate in steel column-baseplate connection

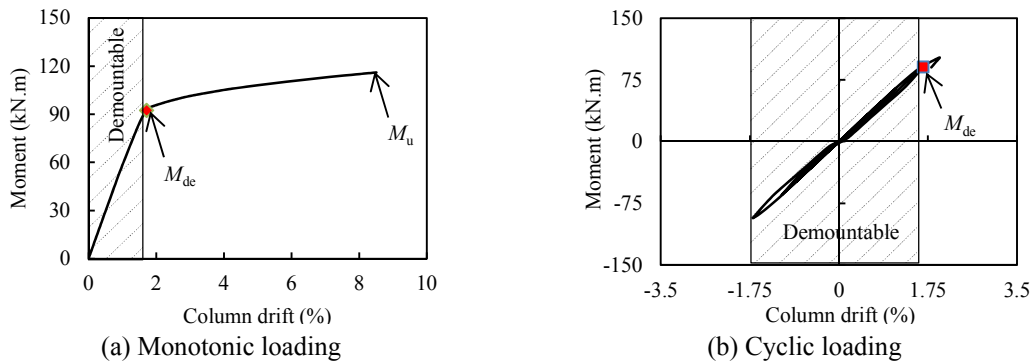


Fig. 20 Demountability of steel column-baseplate connection

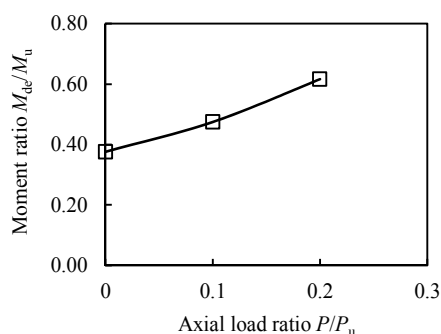


Fig. 21 Effects of axial load on demountability of steel column-baseplate connection

It can be observed from Fig. 20(a) that when the PEEQ is predicted to be less than 0.0015, the column and baseplate can be demounted up to a bending moment of 92.4 kN.m. In Fig. 20(b), the loading and unloading paths of the column-baseplate connection in the first 24 cycles coincide, which indicates that the column-baseplate connection behaves elastically when horizontal cyclic deformation is small. In the 25<sup>th</sup> cycle, large plastic deformation was observed in the baseplate, which results in the demountability of baseplate hard be achieved.

In this section, the finite element analysis of a steel column-baseplate connection was conducted for predicting the amount of plastic deformation in the steel column and baseplate. Test 1 with geometric and material details given in Table 2 and Fig. 7(b) was utilised. It is found that the effects of various parameters on the demountability of a steel column-baseplate connection under monotonic and cyclic loading were largely the same.

#### 4.1 Effects of axial load

Fig. 21 exhibits the effects of axial load on the demountability of the column-baseplate connection.  $P_u$  and  $M_u$  represent the ultimate axial compression and ultimate bending moment capacity of the steel column, and  $M_{de}$  is the moment where large plastic deformation in the column and baseplate occurred. Therefore,  $M_{de}$  is the maximum bending moment, at which steel column and baseplate are demountable and reusable. It can be seen that increasing axial load on top of the column to 20%  $P_u$  can increase the demountability of the column-baseplate connection.

#### 4.2 Effects of baseplate thickness

Four different baseplate thicknesses were used in the parametric study, which include  $t_p = 16.9, 25.4, 38.1$  and  $50.8$  mm. It can be seen from the Fig. 22 that applied moment ratio  $M_{de}/M_u$  increased by 245% and 26.4% when increasing baseplate thickness from 16.9 and 25.4 to 38.1 mm, respectively. However, the maximum bending moment  $M_{de}$  did not change when increasing baseplate thickness from 38.1 to 50.8 mm, which is due to the occurrence of anchor bolt yielding prior to the baseplate yielding.

#### 4.3 Effects of anchor bolt position

Three different anchor bolt positions were used in this analysis which include  $l_1/l_0 = 0.19, 0.45$  and  $0.70$ . It is shown in Fig. 23 that further anchor bolt from the column flange from 32 to 73 mm would increase the maximum bending moment  $M_{de}$  by 8.8%. However, further anchor bolt from

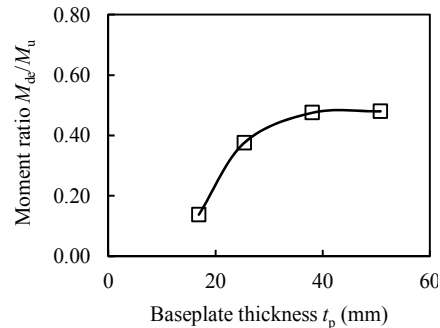


Fig. 22 Effects of baseplate thickness on demountability of steel column-baseplate connection

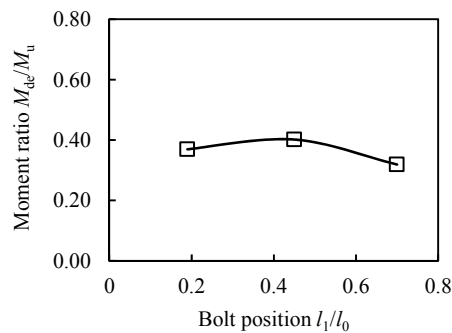


Fig. 23 Effects of anchor bolt position on demountability of steel column-baseplate connection

the column flange from 73 mm to 113 mm decreased the maximum bending moment  $M_{de}$  by 26% to 78.5 kN.m. On the basis of finite element analysis results, in order to delay the yield of baseplate and fully make use of baseplate strength, anchor bolts are ideally positioned in the mid-span between column flange and baseplate short-span edge.

#### 4.4 Effects of anchor bolt diameter

Anchor bolt diameter ranges from 19 to 28 mm were used in this study to examine the effects of bolt diameter on the demountability of column-baseplate connection. It is illustrated in Fig. 24 that varying bolt diameter along did not influence the demountability of the column-baseplate connection significantly, which is due to the yield of baseplate occurred prior to the yield of the anchor bolt. Therefore, the demountability keeps constant, although the ultimate moment capacity of the connection might increase due to the contribution from anchor bolts.

## 5. Comparison of initial stiffness and flexural resistance with Eurocode 3

### 5.1 Concept of Eurocode 3

Eurocode 3 proposed a simplified approach to predict the initial stiffness and bending moment capacity for steel column-baseplate connection, as shown in Fig. 25. In the proposed method, column flange in compression is treated as a T-stub; while the contribution of the partly column

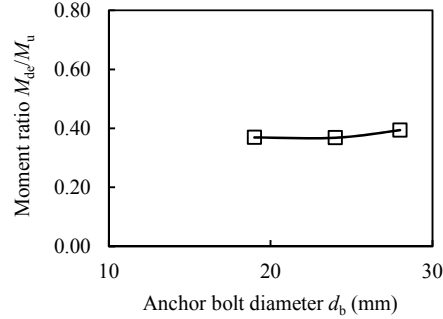


Fig. 24 Effects of anchor bolt diameter on demountability of steel column-baseplate connection

web in compression is neglected. In addition, anchor bolts are the main elements, which provide tension capacity. As stated in Eurocode 3, flexural resistance  $M_{j,Rd}$  of the connection can be expressed as Eq. (3).

$$M_{j,Rd} = F_{t,Rd}Z_t + F_{c,Rd}Z_c \quad (3)$$

in which  $F_{t,Rd}$  is the resistance in tension from the anchor bolts,  $F_{c,Rd}$  is the resistance in compression of the simplified T-stub. As illustrated in Fig. 25,  $Z_t$  and  $Z_c$  are the distances from the column centre line. In addition, resistance in tension and compression can be expressed as

$$F_{t,Rd} = n\phi \frac{f_{ub}A_s}{\gamma_{mb}} \quad (4)$$

$$F_{c,Rd} = f_{jd}b_{eff}L_{eff} \quad (5)$$

where  $n$  is the number of bolts in tension side,  $\phi$  is the safety reduction factor for steel element, taken as 0.9 and  $\gamma_{mb}$  is the safety factor for bolt (1.25). Moreover,  $f_{ub}$  and  $A_s$  are the ultimate stress and cross-section area of the bolt. Foundation bearing strength is represented by  $f_{jd}$ , which accounts for the quality of bedding grout and confinement effects of unloaded concrete;  $b_{eff}$  and  $L_{eff}$  are the effective width and length of the T- stub, respectively.

$$f_{jd} = \beta_j f_c' \sqrt{\frac{A_{c1}}{A_{c0}}} \quad (6)$$

where  $n$  is the number of bolts in tension side,  $\phi$  is the safety reduction factor for steel element, taken as 0.9 and  $\gamma_{mb}$  is the safety factor for bolt (1.25). Moreover,  $f_{ub}$  and  $A_s$  are the ultimate stress and cross-section area of the bolt. Foundation bearing strength is represented by  $f_{jd}$ , which accounts for the quality of bedding grout and confinement effects of unloaded concrete;  $b_{eff}$  and  $L_{eff}$  are the effective width and length of the T- stub, respectively.

$$L_{eff} = \min\{2\pi m, \pi m + W, \pi m + 2e_a, 4m + 1.25e_a, 2m + 0.625e_a + W/2, 2m + 0.625e_a + e_b, b_p/2\} \quad (7)$$

$$b_{eff} = \frac{F_{Ed} + F_{t,Rd}}{f_{jd}(b_c + 2c)} \quad (8)$$

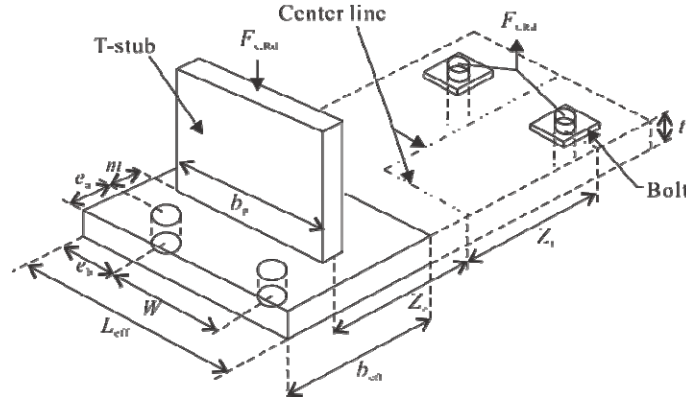


Fig. 25 Simplified approach for column-baseplate connection from Eurocode 3

$$c = t_p \sqrt{\frac{f_y}{3f_{jd}}} \tag{9}$$

with  $f_y$  and  $t_p$  representing the yield stress and thickness of baseplate.

In terms of the bending stiffness calculation, Eurocode 3 also recommended a simplified approach, which comprised stiffness of the compression and tension part. In particular, for the tension part, anchor bolt stiffness and baseplate stiffness were involved, which rely on the existence of prying effect. Prying effect exists when Eq. (10) is satisfied.

$$L_b \leq \frac{8.8m^3 A_s}{L_{eff} t_p^3} \tag{10}$$

where  $L_b$  is the anchor bolt elongation length, which equals to sum of 8 times the nominal bolt diameter, the grout layer, the plate thickness, the washer and half of the height of nut. Calculation of anchor bolt and baseplate stiffness can be followed in Eqs. (11) and (12) for scenarios with and without prying effect, respectively.

$$k_b = \frac{1.6A_s}{L_b}, \quad k_p = \frac{0.85L_{eff} t_p^3}{m^3} \tag{11}$$

$$k_b = \frac{2.0A_s}{L_b}, \quad k_p = \frac{0.425L_{eff} t_p^3}{m^3} \tag{12}$$

$$k_t = \left( \frac{1}{k_b} + \frac{1}{k_p} \right)^{-1} \tag{13}$$

For stiffness of concrete in compression, Eq. (14) can be used

$$k_c = \frac{E_c \sqrt{b_{eff} L_{eff}}}{1.275 E_s} \quad (14)$$

in which  $E_c$  and  $E_s$  are the Young's Modulus of concrete and baseplate, respectively. And bending stiffness can be obtained from Eq. (15).

$$s_{j,ini} = \frac{e}{e + e_k} \frac{E_s z^2}{\left( \frac{1}{k_t} + \frac{1}{k_c} \right)} \quad (15)$$

$$e = \frac{M_{Rd}}{F_{Ed}}, \quad e_k = \frac{k_c z_c - k_t z_t}{k_c + k_t} \quad (16)$$

## 5.2 Comparison of results and discussion

According to the approaches recommended by the Eurocode 3, initial stiffness and bending resistance of a series of column-baseplate connections are calculated and given in Table 4. The corresponding experimental and finite element analysis results are compared with Eurocode 3.

Specimens 8F and 12F were conducted by Picard and Beauliu (1985), pure bending were applied on top of the column. Compared with the experiment and finite element methods, Eurocode 3 overestimates the initial stiffness of specimens 8F and 12F slightly by approximately 8%. For the bending resistance, finite element model produced a 5% higher value compared to experiment, which may be partly due to the ignorance of bolt threads in the developed finite element model. However, bending moment capacity from both the finite element analysis and experiment is smaller than the Eurocode 3.

Stamatopoulos and Ermopoulos (2011) tested specimen SP1 under a combination of flexural bending and axial load. As observed in Table 4, the initial stiffness from experiment is higher than that from finite element analysis, which is mainly due to the unclear of axial loading history. Compared with the predicted values from Eurocode 3, both finite element analysis and experimental results are conservative. However, in terms of the bending resistance, finite element model and experiment agree well with the Eurocode 3.

Tests 1, 5 and 7 were carried out by Gomez *et al.* (2010), where Test 1 was under pure bending and Tests 5 and 7 were subjected to different levels of axial loads. For these tests, anchor bolts were positioned close to baseplate corners, which is a different design compared with other specimens presented in Table 4. The initial stiffness of this column-baseplate connection, which has large spacing between anchor bolts in tension side, was significantly overestimated by the Eurocode 3. Compared to initial stiffness, prediction of flexural bending resistance based on Eurocode 3 is more accurate.

The last four specimens in Table 4 were conducted by Latour *et al.* (2014). Various column sections, baseplate thickness and axial loadings were tested. Furthermore, specimens with column section HEB240 utilised three anchor bolts in both compression and tension side. As observed in Table 4, the initial stiffness and flexural bending resistance from both finite element analysis and experiment are close to the predicted values from Eurocode 3. This is due to the use of more bolts in column-baseplate connection, which consequently render this design closer to rigid connection and match the assumption used in Eurocode 3.

Table 4 Comparison of initial stiffness and moment capacity with Eurocode 3

Specimen	$S_{EC3}$	$S_{FEM}$	$S_{Exp}$	$\frac{S_{j,EC3}}{S_{j,FEM}}$	$\frac{S_{j,EC3}}{S_{j,Exp}}$	$M_{EC3}$	$M_{FEM}$	$M_{Exp}$	$\frac{M_{EC3}}{M_{FEM}}$	$\frac{M_{EC3}}{M_{Exp}}$
8F	12428	11323	11560	1.10	1.08	47.4	41.0	39.0	1.16	1.22
12F	10632	9987	10232	1.06	1.04	45.4	39.2	37.0	1.16	1.23
SP1-0	4601	2316	3200	1.98	1.44	15.4	14.8	13.6	1.04	1.13
SP1-99	5583	2598	4160	2.14	1.35	22.4	20.1	18.6	1.11	1.20
Test 1	16512	5907	5860	2.80	2.82	111.6	98.2	101.6	1.13	1.10
Test 5	20749	12707	11877	1.63	1.75	150.1	140.0	148.9	1.07	1.01
Test 7	25058	16438	15998	1.52	1.57	176.0	162.3	172.0	1.08	1.02
HEA160-15-34	5411	5374	5600	1.01	0.97	32.1	35.1	54.2	0.91	0.59
HEA160-15-233	7348	6408	6120	1.15	1.20	46.5	42.8	83.0	1.08	0.56
HEB240-15-585	19985	19911	20010	1.00	0.99	127.4	106.8	116	1.19	1.10
HEB240-25-585	23247	24495	24506	0.95	0.95	147.7	125.9	129.0	1.17	1.14
Mean				1.48	1.38				1.10	1.03
Standard deviation (SD)				0.60	0.54				0.08	0.23

Concluded from the Table 4, Eurocode 3 generally over-predicts initial stiffness and bending moment capacity of the column-baseplate connection. This over-prediction in terms of initial stiffness is even significantly in the cases where less anchor bolts (semi-rigid connection) and large spacing between anchor bolts are used. Furthermore, the inaccuracy of the predicted initial stiffness from Eurocode 3 might also be attributed to the existence of complex interactions between different components (e.g., anchor bolts and concrete foundation, grout and concrete foundation).

## 6. Conclusions

Steel column-baseplate connections with exposed bolted systems are normally utilised in low to medium rise steel structures to transfer axial forces, shear forces and bending moments to the concrete foundations. In this paper, the proposed finite element model can accurately predict the behaviour of steel column-baseplate connections in terms of initial stiffness and bending moment strength similar to the experimental results.

Comparisons of finite element models and experimental results from the literature showed that the moment-column drift curves in monotonic loading were similar to those in cyclic loading. Furthermore, the failure modes, initial stiffness and ultimate bending moment capacities obtained from the finite element model agree well with the experiments. The validated finite element model was further extended to conduct a parametric study on the steel column-baseplate connection under monotonic and cyclic loading. The effects of four parameters were investigated through finite element analysis by varying one parameter each time.

According to the finite element analysis results from parametric and demountability study, the authors concluded that an increase in axial load generally increases the initial stiffness, ultimate bending moment capacity and demountability of column-baseplate connection. The baseplate

deformation is more significant and ultimate strength in anchor bolt is less under higher axial load, thus the strength of baseplate and anchor bolt can be fully used. Baseplate thickness and anchor bolt diameter played an important role in improving behaviours of column-baseplate connection. Normally, increasing baseplate thickness or anchor bolt diameter increase the initial stiffness, ultimate bending moment capacity and demountability of the steel column-baseplate connection. Nevertheless, this trend decreased when increasing baseplate thickness or anchor bolt diameter alone to a certain value. Furthermore, it is found that arrange anchor bolts in a position, where the distances to column flange and baseplate short-span edge are similar can make the most use of the strength of baseplate. Thereby, the initial stiffness, ultimate bending moment capacity and demountability of the column-baseplate connection can be increased.

Based on the finite element analysis results, it is found that Eurocode 3 over-predicts the initial stiffness and bending moment capacity of steel column-baseplate connections. This over-prediction depends on the design details of steel column-baseplate connection, especially the arrangement of anchor bolts. It can be concluded that more anchor bolts in tension side and small distance between anchor bolts render the steel column-baseplate connection close to rigid constraint, which leads to a closer prediction to the Eurocode 3.

## Acknowledgments

The research described in this paper is financially supported by the Australian Research Council (ARC) under its Discovery Scheme (Project No: DP140102134). The financial support is gratefully acknowledged.

## References

- ABAQUS (2012), Analysis User's Manual, ABAQUS Standard, Version 6.12.
- ACI-318 (2008), Building code requirements for reinforced concrete, ACI; Detroit, MI, USA.
- Armstrong, P.J. and Frederick, C.O. (1966), "A mathematical representation of the multiaxial bauschinger effect", CEBG Report No. RD/B/N 731.
- Aslani, F., Uy, B., Tao, Z. and Mashiri, F. (2015), "Behaviour and design of composite columns incorporating compact high-strength steel plates", *J. Constr. Steel Res.*, **107**, 94-110.
- ATC-24 (1992), Guidelines for cyclic seismic testing of components of steel structures for buildings; Report No. ATC-24, Applied Technology Council, Redwood City, CA, USA.
- Bari, S. and Hassan, T. (2000), "Anatomy of coupled constitutive models for ratcheting simulation", *Int. J. Plasticity*, **16**(3-4), 381-409.
- Carreira, D. and Chu, K. (1985), "Stress-strain relationship for plain concrete in compression", *Am. Conc. I.*, **82**(6), 797-804.
- Chaboche, J.L. (1994), "Modelling of ratchetting: Evaluation of various approaches", *Eur. J. Mech., A/Solids*, **13**(4), 501-518.
- Eurocode 3, Part 1-8 (2005), Design of steel structures – Design of joints, European Committee for Standardisation, Brussel, Belgium.
- Gomez, I.R., Kanvinde, A.M. and Deierlein, G.G. (2010), "Exposed column base connections subjected to axial compression and flexure", Final Report; Presented to the American Institute of Steel Construction, Chicago, IL, USA.
- Grauvilardell, J.E., Lee, D., Hajjar, J.F. and Dexter, R.J. (2005), "Synthesis of design, testing and analysis research on steel column base plate connections in high seismic zones", *Struct. Eng.*, Rep. No. ST-04-02; Department of Civil Engineering, University of Minnesota, Minneapolis, MN, USA.

- Green Building Council of Australia (2009), *Green Star Overview*. URL: [www.gbca.org.au](http://www.gbca.org.au)
- Jaspart, J.P. and Vandegans, D. (1998), "Application of component method to column bases", *J. Constr. Steel Res.*, **48**(2-3), 89-106.
- Jia, L.J. and Kuwamura, H. (2014), "Prediction of cyclic behaviours of mild steel at large plastic strain using coupon tests results", *J. Struct. Eng.-ASCE*, **140**(2), 441-454.
- Kanvinde, A.M., Jordan, S.J. and Cooke, R.J. (2013), "Exposed column base plate connections in moment frames-simulations and behavioural insights", *J. Constr. Steel Res.*, **84**, 82-93.
- Latour, M., Piluso, V. and Rizzano, G. (2014), "Rotational behaviour of column baseplate connections: experimental analysis and modelling", *Eng. Struct.*, **68**, 14-23.
- Li, D., Uy, B., Patel, V.I. and Aslani, F. (2016), "Behaviour and design of demountable steel column-column connections", *Steel Compos. Struct., Int. J.*, **22**(2), 429-448.
- Mirza, O. and Uy, B. (2011), "Behaviour of composite beam-column flush end-plate connections subjected to low-probability, high-consequence loading", *Eng. Struct.*, **33**(2), 647-662.
- Nakashima, S.g1  
(1992), "Experimental behavior of encased steel square tubular column-base connections", *Proceedings of the First World Conference on Constructional Steel Design*, 240-249.
- Picard, A. and Beaulieu, D. (1985), "Behavior of a simple column base connection", *Can. J. Civil Eng.*, **12**(1), 126-136.
- Silvestre, E., Mendiguren, J., Galdos, L. and Argandoña, E. (2015), "Comparison of the hardening behaviour of different steel families: from mild and stainless steel to advanced high strength steels", *Int. J. Mech. Sci.*, **101-102**, 10-20.
- Stamatopoulos, G.N. and Ermopoulos, J.C. (2011), "Experimental and analytical investigation of steel column bases", *J. Constr. Steel Res.*, **67**(9), 1341-1357.
- Targowski, R., Lamblin, D. and Guerlement, G. (1993), "Baseplate column connection under bending: Experimental and numerical study", *J. Constr. Steel Res.*, **27**(1-3), 37-54.
- Uy, B. (2014), "Innovative connections for the demountability and rehabilitation of steel", *Space Compos. Struct.*, Prague, Czech Republic.
- Uy, B., Patel, V.I., Li, D. and Aslani, F. (2016), "Behaviour and design of connections for demountable steel and composite structures", *Structures*. [In Press] DOI: 10.1016/j.istruc.2016.06.005
- Wald, F., Sokolm, Z. and Steenhuis, M. (1995), "Proposal of the stiffness design model of the column bases", *Proceedings of the 3rd International Workshop on Connections in Steel Structures*, Trento, Italy, May.
- Wald, F., Sokolm, Z. and Steenhuis, M. (1996), "Proposal of the stiffness design model of the column bases", *Connect. Steel Struct.*, 249-258.